Localization of Antarctic ice breaking events by frequency dispersion of the signals received at a single hydroacoustic station in the Indian Ocean

Binghui Li and Alexander Gavrilov

Curtin University of Technology, Centre for Marine Sci & Tech, GPO Box U1987, 6845 Perth, WA, Australia
binghui.li@postgrad.curtin.edu.au

Transient acoustic signals from Antarctic ice cracking and breaking events, featuring significant frequency dispersion, were observed at the hydroacoustic stations deployed in the Indian Ocean as part of the International Monitoring System (IMS) of the Comprehensive Nuclear-Test-Ban Treaty. Based on a comparison with numerical predictions, the measured dispersion characteristics were used to estimate the range between ice events and the receiver. Combined with the bearing capability of the IMS stations, these estimates allow us to locate ice events from a single hydroacoustic station. An analysis of range estimation errors due to uncertainty of the measured time-frequency structure of signal arrivals and due to variations of the sound speed profiles was also conducted. The analysis showed that, for the typical ice events, the location accuracy from a single hydroacoustic station was of the same order, as that determined from an intersection of bearings from two remote stations. This localization method was examined by analyzing an ice event detected at both the Cape Leeuwin IMS station and a sea noise logger deployed off the Antarctic shelf.

1   Introduction

In this paper, we investigate the feasibility of localization of Antarctic ice breaking events by a single hydroacoustic station of the hydroacoustic network deployed in the Indian Ocean as part of the International Monitoring System (IMS) the Comprehensive Nuclear-Test-Ban Treaty (CTBT). Data from the HA01 station located about 150 km north-west of Cape Leeuwin in Western Australia [1] are used for analysis. Based on bearing estimation at hydroacoustic stations [2], as well as the signal travel times expected from an acoustic propagation model, the sources of underwater noise can be located using hydroacoustic International Monitoring System (IMS) network, providing the signals are detected by more than one hydroacoustic station with a high signal-to-noise-ratio. The locations of certain intense ice events in the Southern Ocean, including noise making drifting icebergs and collapsing glaciers, were determined using the IMS hydroacoustic network [3，4，5，6]， The network has also been utilized for the purpose of monitoring the distribution of seismic activity in the Indian and Southern Oceans [5, 7, 8].

In our previous studies [6, 9], a specific type of transient signal from Antarctica was identified and localized using the HA01 and H08S hydroacoustic stations. This type of signal is characterized by negative frequency dispersion and is believed to be from ice cracking or breaking events. HO8S is deployed south of the British Indian Ocean Archipelago of Diego Garcia. There are certain problems with event localization using more than one hydroacoustic station. For example, the variations of transmission loss and arrival structure distortion along different propagation paths may make it difficult to detect and identify the arrivals from the same event at different hydroacoustic stations. Also, the sectors of the Antarctic coastline observed from the different IMS stations are different, so that the overlapping parts of these sectors are noticeably smaller than the whole observation sector of Antarctica from the IMS stations in the Indian Ocean. These problems would be partly overcome if the ice events could be located by a single hydroacoustic station. This will require estimation of the range between the events and the receivers in addition to the bearing estimates provided by the IMS hydroacoustic stations with a back-azimuth location accuracy of less than one degree [6, 10].

The range estimation of a remote broadband source could be achieved using a single hydrophone through an analysis of the time-frequency structure of received signals, which fundamentally relates to the modal group velocities, i.e. to the intramodal or intermodal dispersion resulting from the

ducted acoustic propagation in the ocean. For the ocean environment of ATOC experiment [11] with a deep sound channel, Kuperman et al [12] tried to localize the source near the channel axis based on the energy focusing of different modal groups in the time-frequency domain. Ewing and Worzel [13] suggested estimating the range by comparing the total dispersion of a pulse to the total span of group speed possible in the propagation environment. T. C. Yang [14, 15] proposed a method for the measurement of frequency dispersion of broadband pulses that had propagated over a long range. Based on this method, he examined the range estimation technique using frequency dispersion of low order modes in the Arctic acoustic environment with a near-surface sound channel.

In this study our efforts were made toward the range estimation to Antarctic ice events using a single hydroacoustic station, which is based on the measured and modelled frequency dispersion of low-order mode arrival at HA01. Combined with the azimuth, this allows us to implement ice event localization.

2   Frequency dispersion along the propagation path
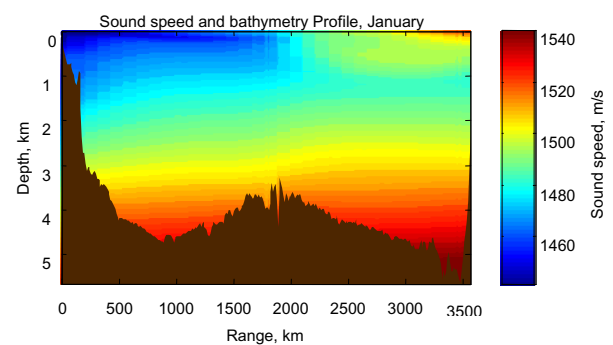
Fig1. The sound speed (in January) and bathymetry profile along the path from the Antarctic coastline [66.783S, 119.5108E] to Cape Leeuwin hydroacoustic station

The propagation of ice signals from the Antarctic coast to the hydroacoustic stations in the Indian Ocean undergo both near-surface sound ducting in the Southern Ocean and deep-water ducting in the SOFAR channel in the temperate ocean regions. These two channels evolve from one to another across the Antarctic Convergence Zone (ACZ) which can be seen in Fig1 at a range of 2000 km from the Antarctic coast. Fig2 shows the typical sound speed profiles, the shape of the first three modes, and the variation of their group velocities with respect to frequency in these two regions. As can be clearly seen from this figure, south of the Antarctic Convergence, modes 1 and 2 have strong

negative frequency dispersion which can be explained by noting that, at higher frequencies, the modal energy is trapped in a narrower duct under the sea surface than that at low frequencies. It should also be noted that there exists an

intermodal dispersion phenomenon, i.e. the higher the mode, the faster it will travel, because its energy will be spread in deeper water
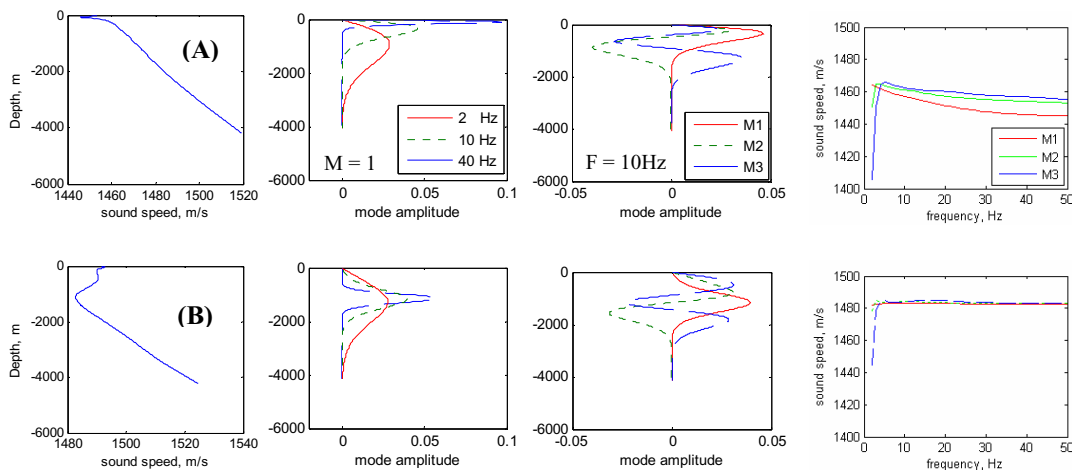
Fig2. The typical sound speed profile in Southern Ocean polar (A) and SOFAR (B) environment, and the corresponding shape of mode 1 at 2, 10, 40 Hz (column 2), shapes of the first three modes at 10 Hz (column 3), and the group velocities of the first three modes (column 4).

layers with higher sound speed. The frequency dispersion curve of mode 1 becomes flat from the frequency of around 35 Hz above which the mode is almost fully trapped within the near-surface channel. Modes 2 and 3 exhibit a relatively weaker dispersion effects in comparison with mode 1.

For the propagation over the SOFAR channel section, none of the first three modes undergo either intermodal or intramodal dispersion at frequencies above 5 Hz. The frequency range below 5 Hz was not considered in this study, because it is below the cut-off frequency for modal propagation along the shallow water section of the propagation path over the Antarctic continental shelf.

3   Ice event range estimation from a single hydroacoustic station

3.1   The time-frequency structure of signal arrivals from ice events

The high-resolution measurement of the arrival time-frequency structure of dispersive signals is critical for the range estimation. Under the uncertainty principle, if there is no additional confining information about the arrival structure of signals, the frequency resolution could not be higher than the reciprocal of the time duration. So, for the conventional time-frequency structure measurement, one has either to sacrifice frequency resolution in order to achieve the required time resolution, or to improve the frequency resolution at the cost of the time resolution by elongating the time window within which the measured frequency may not necessarily correspond to the instantaneous frequency at the centre of the selected signal section.

Based on the prior theoretical knowledge of the signal spectrum expected for different arrival times, T. C. Yang [15] proposed a method for high-resolution determination

of the mode frequencies as a function of arrival time. For the condition of the range-independent Arctic Ocean environment, the low frequency pulse signals propagated over long ranges consist of discrete normal modes, and the power spectrum of modal signals within finite time intervals $2\Delta t$ can be approximated as:

$$\left| \sin(\omega - \omega_n)\Delta t /(\omega - \omega_n) \right|^2 \qquad (1)$$

Where ω_n is the instantaneous frequency of mode *n*. The length $2\Delta t$ of the sampling intervals is subject to certain bound conditions. The stationary phase approximation was used in the derivation of the theoretical power spectrum in a range-independent environment. The derivation procedure, as well as the result similar to Equation (1) can be adapted to range-dependent conditions if the acoustic mode propagation is nearly adiabatic, as that expected for the propagation path from the Antarctic coastline to HA01, where the mode coupling effect is small [6]:
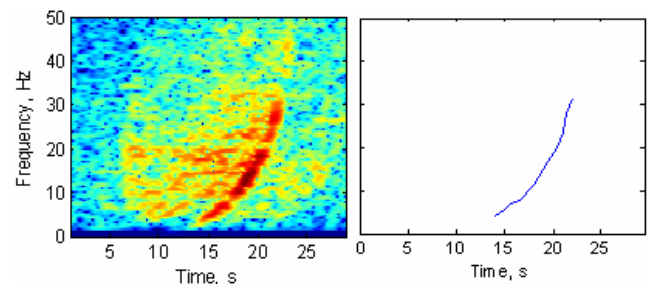
Fig3. The spectrogram of an ice event received at HA01 with back-azimuth of 160.67 degree (left panel) and its fine time-frequency structure measured with a resolution of 0.5 Hz (right panel).

The process of time-frequency structure measurement applied to transient signals from ice events was split into the following steps:

1) Divide the signal arrivals into a series of time segments bounded according to inequality (3) given in reference [15];

2) Compute the power spectrum for each time segment extended by adding zeros in order to achieve the required frequency bin size, which was set as 0.5 Hz;

3) Make a comparison of the measured and theoretically predicted spectra by shifting the assumed mode frequency ω_n of the theoretical spectrum around the peak values of the measured spectrum, along with slightly changing the length of time segments within the bounds that the length of the time segment is subject to. The mode frequency is determined when the deviation of the integral of the theoretical spectrum from that of the measured one is less than 10% , suggested in reference [15] for the frequency width $|\omega - \omega_m| < \pi / 2\Delta t$; and finally

4) Plot mode frequencies against the central time of each segment as the measured time-frequency structure of the arrivals.

Fig3 shows the spectrogram of a typical transient ice event received at HA01, and the fine time-frequency structure derived through the above procedure.

3.2   Procedure for range estimation

Range estimation for ice events can be conducted by best fitting of measured and modelled time-frequency structure. The frequency dispersion of different modes was modelled using a range-dependent adiabatic normal mode model. The monthly sound speed profiles were calculated from the analysed and gridded CTD data available from the NODC World Ocean Atlas (WOA) 2005 climatology oceanographic data http://www.nodc.noaa.gov/OC5/WOA01/pr_woa01.html), and the bathymetry profiles were taken from the ETOPO2 Global 2-Minute Gridded Elevation Data (http://www.ngdc.noaa.gov/mgg/fliers/01mgg04.html). The mode frequency dispersion was calculated on a 10-km grid along the path from the Antarctic coast to the receiver along the back-azimuth to the ice event determined at HA01. During the curve fitting process, we are looking for the least mean square (LMS) difference between measured and modelled arrival times of different frequencies of mode one. Both measured and modelled arrival times are relative to the measured arrival time of the first observed arrival. Therefore the estimated range from HA01 to the event R_{LMS} can be expressed as the inverse function of the LMS fitting of the modelled and measured relative arrival times of nth mode T_{LMS} regarding mode frequency ω_n:

$$R_{LMS} = f^{-1}(T_{LMS}(R_{LMS}(\omega_n))) \qquad (2)$$

$$T_{LMS}(R_{LMS}(\omega_n)) = f(R_{LMS})$$
$$= \min[(\sum_k (T_n^{ME}(r(\omega_{n,k})) - T_n^{MO}(r(\omega_{n,k})))^2] \qquad (3)$$

Where $\omega_{n,k}$ is the nth mode frequency within the k-th arrival section, $T_n^{ME}(r(\omega_{n,k}))$ and $T_n^{ME}(r(\omega_{n,k}))$ are measured and modelled relative arrival times, at range of r, for n-th mode frequency of the k-th arrival section respectively. The error of range estimation could appear either from the process of time-frequency structure measurement of arrivals or from errors of frequency dispersion modelling. The mode frequency resolution in the measurement of the time-frequency structure is set to be 0.5 Hz in this study. Therefore the error of range estimation appearing from the time-frequency measurements can be estimated by adding the resolution value to the measured mode frequency:

$$\Delta R_{LMS} = f^{-1}[T_{LMS}(R_{LMS}(\omega_n))] - f^{-1}[T_{LMS}(R_{LMS}(\omega_n'))] \qquad (4)$$

Where $\omega_n' = \omega_n \pm 0.5$

3.3   Case studies
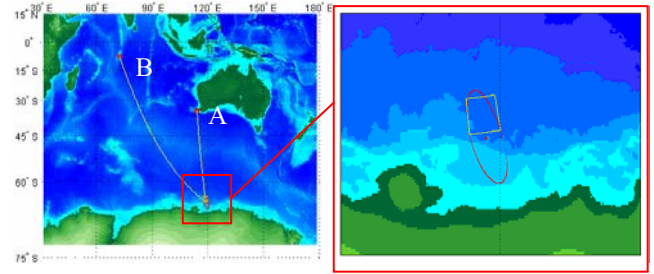
Fig4. The ice event location (left panel) and a comparison of its errors (right panel) estimated from two stations, HA01 (A) and H08S (B) (red), and only from HA01 (yellow) using range estimates based on signal dispersion.

Two independent case studies are considered in this section to verify the feasibility of proposed range estimation of Antarctic ice events based on the frequency dispersion. One of the signals from Antarctic ice events was received at both HA01 and H08S station on the 17th of January 2003. Its spectrogram observed at HA01 and the measured time-frequency structure are shown in Fig3. A comparison between the location errors expected for the source location from the two stations and only from HA01 was shown in Fig. 4. In the right panel, the red dot shows the intersection of two back-azimuths from both stations. The 90% confidential ellipse of event location is indicated by the red line. This confidence ellipse was calculated assuming that the errors of bearing estimates are Gaussian distributed and have a standard deviation of half-degree for both stations. The region enclosed by the yellow rectangle is the area the event is expected to be in, which is based on a 0.5- degree azimuth error of bearing from HA01, and the variation of the 0.5 Hz mode frequency measurement. The sound speed profile used in the model is from the January WOA05 climatology. It can be clearly noticed that the location estimate from a single hydroacoustic station has errors comparable to the location from two remote stations.

The error of the range estimation can also result from the modelling process, especially from the uncertainty of the sound speed profiles used for modelling. The monthly sound speed profiles derived from the objectively analysed oceanographic data are the mean values averaged over the period of corresponding month and only reflect the large-
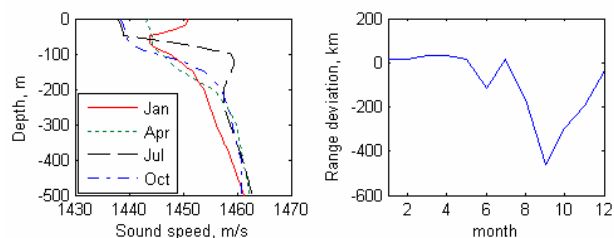
Fig5. The typical monthly sound speed profile in the top 500-m water layer in four different seasons in the Southern Ocean (left panel), and the difference between the range estimates to the ice event obtained through dispersion inversion of the signal at HA01 and that obtained by the intersection of two azimuths of HA01 and H08S stations (right panel).

scale variations of the acoustic propagation environment. Regarding the context of the long-range propagation in this study, we ignore the effects of smaller scale variations and only investigate the variation of range estimates due to the selection of different monthly SSPs. The left panel of Fig.5 shows the typical monthly sound speed profiles in the Southern Ocean beyond ACZ which clearly reveals that the near-surface acoustic propagation channel changes considerably with seasons. The deviation of range estimates from the original location shown in Fig. 4 with change of the monthly SSP used for modelling is shown in the right panel of Fig.5. The deviation of range estimates is significant: in this particular case, the maximum error is about - 400 km, if the winter SSP is used to predict the range to this ice event which actually happened in summer. This takes place because the effect of near-surface ducting of acoustic propagation on frequency dispersion is considerably stronger in winter than in summer. Therefore it is essential to use the corresponding monthly SSP when performing the range estimation for Antarctic ice events.

Fig 6. (a) Signals from the same series of transient events recorded on the Antarctic sea noise logger (top) and at HA01 (bottom), and waveforms (b) and spectrograms (c) of the first signal in the series of events at the logger (top) and HA01 (bottom).

An autonomous sea noise logger was installed in 2004 on the seafloor in the water depth of nearly 3,000 meters on the Antarctic continental slope about 200 km north of Cape Poinsett, close to Casey research station. The logger recorded sea noise during nearly one year [16] and several ice events were detected and identified as those also observed at the HA01 station 3220 km away. The left panel of Fig 6 shows a series of events detected at both the Antarctic logger (top panel) and HA01 station (bottom panel). The right panel shows the waveforms of the first event at the two receivers, along with their spectrograms, of which the one at HA01 station reveals strong frequency dispersion with several discrete arrivals. The time-frequency structure of the latest arrival of mode 1 within the frequency band from 5 to 12 Hz and the time interval of about 3 seconds was used for estimation of range to this event. The location of the initial sound emission was determined using the range estimate through dispersion inversion and the back-azimuth measurement from HA01 station, which was 182.2 degree. A comparison between the modelled and measured arrival structures of the signal received at the Antarctic logger was made based on the estimated location of the sound source, which is nearly 180km away from the Antarctic logger. The depth of sound emission can be determined from the travel difference of the signals that comprise pairs of arrivals with and without reflection from the sea surface near the source. For this particular event, the source depth was estimated to be about

350 metres. Fig7 shows the measured and modelled relative arrival times of individual arrivals (left panel) and the arrival intervals (right panel). The modelled and measured values agree with each other quite well. Even after more than ten reflections from the sea surface and seafloor, the difference between modelled and measured propagation times relative to the first arrival still remains less than one second for a distance of 180km between logger and estimated event location. Also, the arrival intervals of impulses for both modelled and measured signal structures exhibit almost the same trend, even though small deviations appeared on the curves. This case study verifies that the actual location of the sound emission should not have a large deviation from that estimated by frequency dispersion effect.
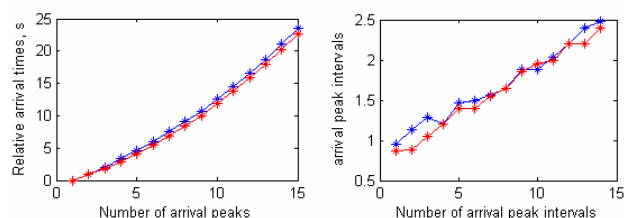
Fig7. Comparison between modelled (blue colour) and observed (red colour) relative peak arrival times (left panel) and arrival peak intervals (right panel).

4   Conclusion and discussion

Intermodal and intramodal frequency dispersion effects due to the near-surface acoustic propagation across the Southern ocean beyond the ACZ, and that through the SOFAR channel were analyzed in this paper in order to investigate the feasibility of range estimation for Antarctic ice events detected at the HA01 hydroacoustic station. The fine time-frequency structure of received signals was determined with a frequency resolution of 0.5 Hz. From the two case studies, it was revealed that the location accuracy of ice events estimated from the frequency dispersion effect for the signal received at HA01 has the same order as that estimated from the intersection of two bearing measurements from two remote stations. This conclusion was also examined by verifying the range estimation of the Casey event through analysis of the structure of arrival pulses at the Antarctic logger.

The modeling of acoustic propagation from Antarctica to the hydroacoustic station was performed using the adiabatic approximation and the sound sources were assumed to emit short pulses in this study. If there exists strong mode coupling along the acoustic propagation path, or the sound sources are not impulsive or the transfer function varies significantly in the frequency domain, we need a different approach to measure the time-frequency structure of arrivals. In addition, the accuracy of range estimation strongly depends on the frequency band and duration of the analyzed signals. The results of this study were obtained for the signals which had the frequency bandwidth at least 7 Hz wide lying between 5 Hz and 35 Hz. The feasibility and accuracy of range estimation from the signals of different frequency bands need to be additionally investigated.

Acknowledgments

References

[1] Lawrence, M. W, "Overview of the hydroacoustic monitoring system for the Comprehensive Nuclear-Test Ban Treaty", *J. Acoust. Soc. Am* 105: 1037 (1999)

[2] Edoardo Del Pezzo and F. Giudicepietro, "Plane wave fitting method for a plane, small aperture, short period seismic array: a MATHCAD program" *Computers & Geosciences* 28: 59-64 (2002)

[3] Emily Chapp, DelWayne, R.Bohnenstiehl, and Maya Tolstoy, "Sound-channel Observations of Ice-generated Tremor in the Indian Ocean", *Geochemistry, Geophysics and Geosystems* 6 (2005)

[4] Jeffrey A. Hanson and J. Roger Bowman, "Methods for monitoring hydroacoustic events using direct and reflected T waves in the Indian Ocean", *Journal of Geophysical Research* 111, B02305, doi: 10.1029/2004JB003609 (2006)

[5] Jacques Talandier, Olivier Hyvernaud, Dominique Reymond, Emile A. Okal, "Hydroacoustic signals generated by parked and drifting icebergs in the Southern Indian and Pacific Oceans", *Geophys. J. Int.* 165: 817-834 (2006)

[6] B. Li and A. N. Gavrilov, "Hydroacoustic observation of Antarctic ice disintegration events in the Indian Ocean". *Proceedings of ACOUSTICS 2006*, Christchurch, New Zealand (2006)

[7] Jeffrey A. Hanson and J. R. Bowman, "Indian Ocean ridge seismicity observed with a permanent hydroacoustic network." *Geophysical Research Letters*, Vol.32, L06301, doi:10.1029/2004FL021931 (2005)

[8] Frank M. Graeber and Pierre-Franck Piserchia, "Zones of T-Wave excitation in the NE Indian Ocean mapped using variations in backazimuth over time obtained from multi-channel correlation of IMS hydrophone triplet data", *Geophys. J. Int.* 158: 239-256 (2004)

[9] Gavrilov, A. N. and G. Vazques, "Detection and Localization of Ice Rifting and Calving Events in Antarctica Using Remote Hydroacoustic Stations", *Proceedings of ACOUSTICS 2005*, Busselton, Western Australia (2005).

[10] Binghui Li, Alexander Gavrilov and Alec Duncan, "Bearing calibration of the Cape Leeuwin hydroacoustic station", *Proceedings of ACOUSTICS 2008*, Geelong, Victoria (2008). (abstract accepted)

[11] ATOC Consortium, "Ocean climate change: Comparison of acoustic tomography, satellite altimetry, and modelling", *Science* 281: 1327-1332 (1998)

[12] W. A. Kuperman, G. L. G' Spain, and K. D. Heaney. "Long range source localization from single hydrophone spectrograms", *J. Acoust. Soc. Am* 109(5): 1935-1943 (2000)

[13] M. Ewing and J. L. Worzel, "Long-range sound transmission", *Geo. Soc. Am*., Memoir 27 (1948)

[14] Yang, T. C., "Dispersion and ranging of transient singals in the Arctic Ocean", *J. Acoust. Soc. Am* 76(1): 262-273 (1984)

[15] Yang, T. C. "A method for measuring the frequency dispersion for broadband pulses propagated to long ranges", *J. Acoust. Soc. Am* 76(1): 253-261 (1984)

[16] Gedamke J., Australian Antarctic Division (personal communication)